12-25-2007

Imaging Thermal Stratigraphy in Freshwater Lakes Using Georadar

John H. Bradford
Boise State University

Cody R. Johnson
Utah State University

Troy Brosten
Boise State University

James P. McNamara
Boise State University

Michael N. Gooseff
Pennsylvania State University

 DOI: 10.1029/2007GL032488

Imaging thermal stratigraphy in freshwater lakes using georadar

John H. Bradford,[1] Cody R. Johnson,[2] Troy Brosten,[1] James P. McNamara,[1]
and Michael N. Gooseff[3]

Received 31 October 2007; accepted 20 November 2007; published 25 December 2007.

[1] Thermal stratification exerts significant control over biogeochemical processing in freshwater lakes. Thus, the temporal and spatial distribution of the thermal structure is an important component in understanding lake ecosystems. We present the first reported observations of lake thermal stratification from surface based georadar measurements acquired over two small freshwater lakes. This method is very useful because it can provide rapid acquisition of 2D or 3D lotic stratification. **Citation:** Bradford, J. H., C. R. Johnson, T. Brosten, J. P. McNamara, and M. N. Gooseff (2007), Imaging thermal stratigraphy in freshwater lakes using georadar, *Geophys. Res. Lett.*, *34*, L24405, doi:10.1029/2007GL032488.

1. Introduction

[2] Thermal stratification of lakes depends largely on energy input at the surface. Because total surface energy varies as a function of air temperature, wind, solar input, and the temperature of stream and rainwater input, the thermal structure of a lake is a dynamic system that may reach quasi-steady state conditions for short periods. A typical scenario during the summer season is wave-induced mixing of a warm surface layer with a deeper cold layer. At steady state, these layers are approximately isothermal and separated by the thermocline, a distinct, high thermal gradient boundary. Here, we present the first reported georadar images of thermal boundaries in two small freshwater lakes. These images show considerable spatial variability in the distribution of water temperature and illustrate that the georadar method is a tool that can enhance our understanding of thermal variability in lakes. This new application of the georadar method provides the ability to produce detailed images of thermal variability as a function of time and space, which in turn can provide valuable input in developing an understanding of lake and lake ecosystem response to climactic variability.

[3] The thermal structure and dynamics drive many biochemical and ecological processes in lakes [*MacIntyre et al.*, 2006]. During thermal mixing benthic sediments are re-suspended [*Hawley and Lee*, 1999], and dissolved oxygen concentrations, nutrients, and organic matter are typically uniform throughout the water column [*Wetzel*, 2001]. Following thermal stratification, lakes are vertically separated by the thermocline into discrete epilimnetic and hypolimnectic habitats [*Hutchinson*, 1957]. Hypolimnetic waters typically become nutrient enriched as settling organic matter is mineralized, while dissolved oxygen levels are depleted during aerobic respiration. Epilimnetic waters stay well oxygenated, but become nutrient depleted as relatively high levels of primary productivity consume inorganic nutrients [*Rimmer et al.*, 2005].

[4] Thermocline depth also determines habitat availability to open water species. Zooplankton are more tolerant than fish to low dissolved oxygen concentrations [*Wright and Shapiro*, 1990], and migrate to the hypolimnion as a refuge from predation. Some species of zooplankton use the thermocline as a vertical habitat boundary between populations [*Johnson et al.*, 2007]. Habitat partitioning by zooplankton alleviates interspecific competition [*Leibold and Tessier*, 1997], while cold stenothermic species of zooplankton continuously occupy the hypolimnion [*Makino et al.*, 2003].

2. Method

[5] The typical approach to measuring the thermal structure of lakes is to make temperature measurements along a vertical profile at one or more locations. This approach provides good vertical resolution but provides little indication of lateral continuity. To measure lateral changes, a thermometer may be towed while alternately raising and lowering the instrument in a sawtooth pattern, sometimes referred to as a TOW-YO or YO-YO system. This approach is limited in both lateral and vertical resolution as well as the volume of water sampled. Although reports in the literature are limited, acoustic methods have proven effective in the imaging of lateral water column variability. For example, *Thorpe and Brubaker* [1983] related acoustic backscatter in the 102 kHz range to thermal microstructure while *Imberger* [1985] attributed acoustic reflections in a fresh water lake to air bubbles, clay particles, organisms and density microstructure. *Holbrook et al.* [2003] showed that low frequency (10–100 Hz) acoustic reflection techniques are capable of imaging the thermohaline structure in the open ocean. High frequency acoustic methods (100–500 KHz) are commonly used for imaging shallow fine structure in the ocean environment that may be a combination of zooplankton or temperature related backscattering [*Haury et al.*, 1979; *Wiebe et al.*, 1997]. *Jonas et al.* [2003] measured thermal convection currents in a small fresh water lake using an acoustic Doppler current profiler. However, to the best of our knowledge, the use of georadar techniques to image thermal structure in fresh water systems has not been previously reported in the literature.

[6] At frequencies above about 200 MHz, dipole relaxation of water molecules dominates electromagnetic (EM) wave propagation through fresh water [*Olhoeft*, 1981]

[1]Department of Geosciences, Boise State University, Boise, Idaho, USA.
[2]Department of Watershed Sciences, Utah State University, Logan, Utah, USA.
[3]Department of Civil and Environmental Engineering, Pennsylvania State University, University Park, Pennsylvania, USA.

0094-8276/07/2007GL032488$05.00

resulting in highly non-stationary waveforms and rapid signal attenuation. However, at low frequencies (10–100 MHz) EM waves exhibit relatively low dispersion and attenuation in fresh water, and this frequency range is well suited to a variety of water-borne imaging applications [e.g., *Bradford et al.*, 2005; *Haeni*, 1996; *Schwamborn et al.*, 2002]. Imaging thermal boundaries as radar reflectors depends on the temperature transition occurring over a vertical distance that is significantly smaller than a wavelength at the peak operating frequency of the radar system. At 10–100 MHz, the corresponding wavelengths in fresh water are 3.25–0.325 m respectively. Given an approximate vertical resolution limit of ¼ wavelength, it should be possible to resolve changes that occur over a few to tens of cm vertically, but temperature changes that occur more gradually may not generate a reflection. Modern georadar systems are lightweight and have relatively low power requirements making transport and deployment feasible and low cost, even for remote field locations.

3. Field Experiments

[7] We initially observed laterally coherent radar reflections within the water column of fresh water lakes while conducting lake-bottom sediment surveys. Working from the hypothesis that the reflections were generated by the lake thermocline, we subsequently designed an experiment to test this interpretation at Toolik Lake, in the northern foothills of the Brooks Range in the Alaskan Arctic. Toolik Lake is a small kettle lake with a surface area of 1.5 km^2, mean depth of 7.1 m, maximum depth of 25 m [*MacIntyre et al.*, 2006], and multiple subbasins. For this experiment we used a commercial pulsed georadar system with linear dipole antennas operating at a dominant frequency of approximately 50 MHz with a corresponding wavelength in water of 0.65 m. The radar antennas were mounted on small rubber raft and towed approximately 5 m behind a 4 m aluminum fishing boat. Data processing included background removal by median trace subtraction, high pass filter (DEWOW) in the time domain using a median filter with time gate equal to twice the characteristic period, and a spherical spreading gain correction.

[8] Control for the experiment was maintained by acquiring vertical profiles of temperature, electric conductivity, turbidity, dissolved oxygen, pH, and chlorophyll (a proxy for phytoplankton biomass) near the center of the georadar transect immediately after radar data acquisition. The radar reflectivity is affected by electric conductivity and dielectric permittivity. The only direct control measure was then electric conductivity, however each of the other 5 measured parameters has the potential to influence either the dielectric permittivity or conductivity so we term these indirect parameters. Measurements were made every 0.5 m vertically with a Hydrolab^{TM} submersible sensor, allowing the instruments to equilibrate for ~1 min prior to recording the data point. We estimate vertical precision of the measurements at ~0.25 m because of wave motion.

[9] We acquired the test radar profiles over an approximately 20 m deep subbasin. We acquired Line 1 on 8/8/2005, at approximately 7:00 p.m. AKDT after two days of relatively high winds. The average wind speed at Toolik Field Station, located on the northeast shore, during the 8 hr period preceding data acquisition was 4.65 m/s and the average temperature over the same period was 17.1 C. We expected these surface conditions to push the thermocline to a relatively deep position due to mixing in the upper part of the lake. In the georadar profile (Figure 1a), a well-defined, laterally continuous radar reflection is present in the water column at a depth of 10 m. This reflection corresponds very well to the thermocline depth determined from temperature measurements (Figure 1b).

[10] To isolate the source of the reflectivity we considered the observations of electric conductivity, turbidity, pH and chlorophyll and concluded that there was no significant systematic change at 10 m in any of these parameters that could explain the reflectivity (Figure 2). Further, both bubbles and zooplankton are known to cause acoustic reflections in the water column. The zooplankton community in Toolik Lake is dominated by two species of copepod, *Cyclops scutifer* and *Diaptomus pribilofensis*; these two species comprise >90% of the zooplankton density in Toolik Lake. The two species use the thermocline as a habitat boundary, however, while the thermocline divides the two species, the highest densities of *C. scutifer* and *D. pribilofensis* are found at depths either much deeper or shallower than the thermocline, respectively [*Johnson et al.*, 2007]. Although we did not specifically sample for bubbles, aeration of the water in horizontal bands would likely be biologically produced, either by phytoplankton or zooplankton. Based on the analysis above, it is unlikely that bubbles were present at the thermocline. We conclude that neither zooplankton nor bubbles were likely responsible for the radar reflectivity in this case.

[11] Lake temperature, however, decreases from 12.6 C in the surface layer to 5.5 C in the deep layer (Figure 1b). Using the temperature dependent, dual Cole-Cole relaxation model given by *Olhoeft* [1981], these temperatures correspond to relative dielectric permittivity values of 82.8 and 84.9 respectively (Figure 1b). Assuming that the reflection is generated entirely by the temperature change and that reflectivity in this case is a function only of dielectric permittivity contrast results in a reflection coefficient of −0.00596. Further assuming a lake bottom relative dielectric permittivity of 39.0 based on measurements at nearby ponds [*Bradford et al.*, 2005] yields a water bottom reflection coefficient of 0.192.

[12] The ratio of the water bottom reflection coefficient to the thermocline reflection coefficient then should be equal to the amplitude ratio of the thermocline reflection and the water bottom reflection in data corrected for spherical spreading. The measured water bottom to thermocline amplitude ratio is 24 ± 12 while the predicted reflection coefficient ratio is 32.2. The above analysis indicates that the reflectivity at 50 MHz is primarily a function of temperature.

[13] We acquired Line 2 on 8/10/2005 at approximately 7:00 p.m. AKDT, after a period of relatively calm weather (Figure 1c). The average wind speed during the 8 hrs preceding data acquisition was 1.72 m/s with an average temperature of 21.7 C. The georadar data clearly show a transition of the thermal stratigraphy with the presence of two distinct zones of reflectivity that correspond to the development of two primary thermal boundaries. The shallower boundary is at a depth of ~2 m and the deeper

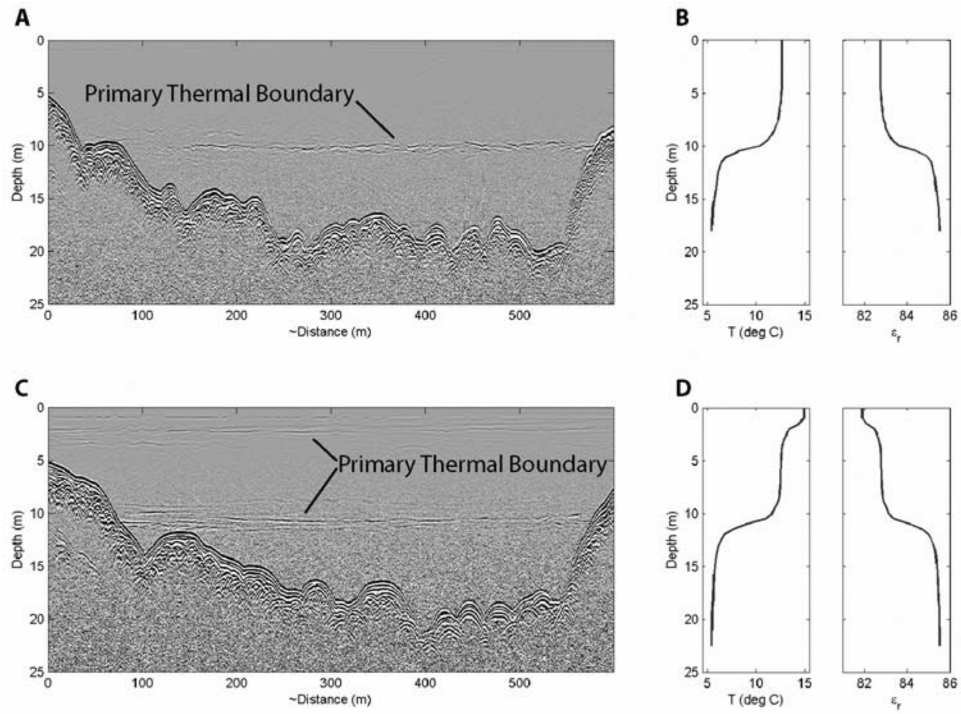

Figure 1. Georadar profiles acquired on Toolik Lake with temperature data and computed permittivity profiles. (a) Line 1 acquired on Toolik Lake after two days of strong winds. The thermocline is at a depth of ~10 m. (b) Temperature data taken at 410 m along the profile, and computed real part of the relative dielectric permittivity. (c) Line 2 acquired 2 days after the profile in Figure 1a and after 1 day of calm weather. The thermal structure has split into three primary layers in response to the change from high energy surface conditions to low energy conditions. (d) Temperature data and computed relative dielectric permittivity at 390 m along the georadar profile in Figure 1c. The radar data show substantial lateral heterogeneity in thermal structure and record discrete thermal boundaries near the thermocline that are not evident from the temperature measurements.

boundary is consistent with the previous thermocline at a depth of 10 m. The temperature profile shows that the lake is divided vertically into three different temperature regimes (Figure 1d). We interpret this structure as transitional as the lake responds to the decrease in surface energy input. Note that the radar data show an intricate and laterally variable distribution of thermal packages separated by distinct boundaries. The measured temperature profile fails to capture the fine-scale vertical variability. While it may be possible to measure the vertical temperature distribution with greater precision, the lateral variability is much more difficult to capture with conventional temperature measurements. Lateral variability occurs over scales from meters to tens of meters and it would not be practical to deploy an adequate number of temperature sensors to fully capture the lateral variability over large distances. This observation highlights the real strength of the georadar method, that radar can provide detailed lateral continuity between vertical temperature profiles.

[14] In a second example, we acquired data on Bull Trout Lake in the Sawtooth Mountains near Boise, Idaho, USA. Bull Trout Lake is a small mountain lake formed by a moraine dam. The lake covers 0.3 km^2, has a mean depth of 4.3 m, and maximum depth of 15.0 m [*Arp et al.*, 2006]. While lacking detailed water column control measurements, we did acquire several temperature measurements. At the time of data acquisition, surface water of the lake was 15.6 C and at a depth of 15 m the temperature was 12.1 C. We also measured the temperature of the inlet stream, approximately 1 km upstream of the shoreline, over a 3 day period. The mean temperature of the stream was 7.0 ± 2.7 C with the variability primarily due to diurnal variation. While there was likely some warming of the inlet stream water between the measurement location and the lake inlet, it is clear that the stream water was substantially cooler than the lake water.

[15] This temperature contrast is clearly evident in the georadar data where the cool inlet stream water is seen entering the lake from the right hand side of the profile, then gradually sinking toward the left (Figure 3, zone 1). Mixing cells are evident as a set of lakeward progressing clinoforms along the inlet thermocline between 700 and 1100 m (Figure 3, zone 2). From 100 to 700 m, there is no evidence of these small scale mixing cells, and the thermocline is evident as a distinct reflector with significantly higher amplitude. It appears that the inlet current continues across the entire lake, reaching a maximum depth of 3 m at the left hand bank. Current waves reflected from the left shore appear to form below 3 m, with several large scale mixing cells forming between depths of 3 and 8 m (Figure 3, zone 5). In all, there were at least 6 distinct thermal zones separated by discrete boundaries within the lake at the time of data acquisition – the boundaries are clearly evident in the georadar data between 600 m and 1100 m (Figure 3)

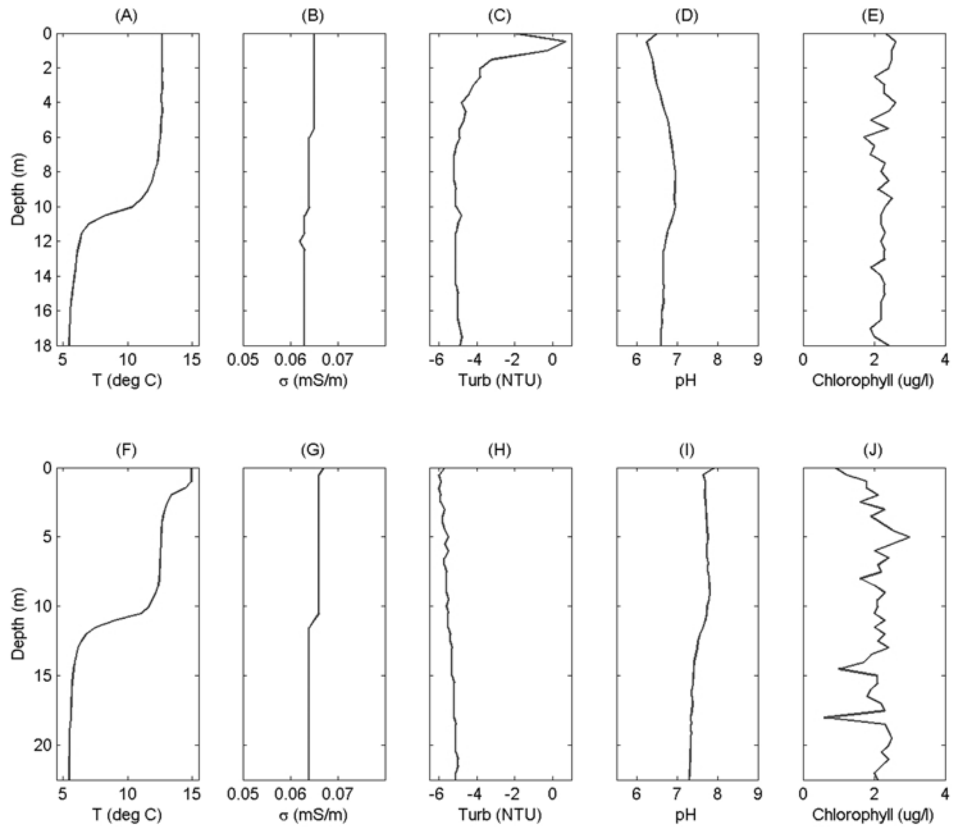

Figure 2. Measured properties in Toolik Lake (a)–(e) after a period of high winds and (f)–(j) 2 days later after the weather had remained relatively calm for several hours. High winds created a deep mixed zone pushing the thermocline to a depth of approximately 10 m (Figure 2a). None of the other measured properties show a trend consistent with thermal gradient. After the calm period, the lake developed 3 distinct temperature layers (Figure 2f). We interpret this as a transitional stage as the temperature profile adjusts to the change in surface energy input. Again no other properties show a trend consistent with the thermal gradient, aside from a small change in electric conductivity at the 10 m boundary. The conductivity change is too small to explain the radar reflectivity.

although the driving mechanisms leading to formation of zones 3, 4, and 6 are not clear. Although the character and driving mechanism differ from that at Toolik Lake, the thermal stratigraphy imaged using georadar again shows complex and laterally variable thermal structure that would be difficult to capture with temperature measurements alone. Our interpretation should be taken with the caveat that lacking control measurements such as turbidity, it is possible to attribute the observed reflections to physical property changes other than temperature. However, given the large difference in temperature between the inlet stream and the lake water coupled with our observations at Toolik Lake, the interpretation that temperature related dielectric permittivity changes dominate the observed georadar response is reasonable.

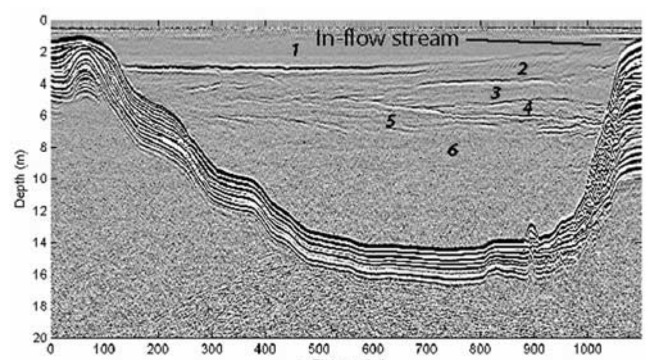

Figure 3. Georadar profile acquired at Bull Trout Lake. The cool inlet stream enters the lake to the right of the profile. These cool waters evidently sink as the cool water propagates across the lake. Mixing is clearly evident as sets of closely spaced leftward dipping clinoforms near the inlet (from 700 m to 1000 m). The stratigraphy beneath the primary thermocline (at ∼2–3 m depth) shows lateral and vertical complexity suggesting multiple mixing cells separated by discrete thermal boundaries. Numbered regions indicate our interpretation of 6 distinct thermal zones within the lake. The processing flow was the same as that for the data in Figure 1.

4. Conclusions

[16] For the first time, we have demonstrated that it is possible to image detailed thermal stratigraphy in freshwater lakes using a commercially available georadar system. With antennas operating at a peak frequency of 50 MHz, we were able to image subtle and laterally variable contrasts in thermal structure that might be missed using conventional temperature measurements. The imaged thermal stratigraphy

is merely a snapshot in time of a dynamic system, but the radar data can be acquired at a rate of several km/hr enabling coverage of large areas over a relatively short period of time. When linked with a precise positioning system it should be possible to capture the three-dimensional temporal evolution of thermal stratigraphy in small fresh water lakes. The radar images are comparable to what might be imaged using acoustic methods as the two wave types are similarly sensitive to temperature changes. Radar then provides an alternative to acoustic imaging, or may provide complimentary information as the physical mechanisms driving the two methods differ entirely. Portability, ease of use, and low power requirements make radar an attractive field tool that has the potential to measure detailed thermal structure leading ultimately to better understanding of the physical processes that govern lake ecosystems.

[17] **Acknowledgments.** This material is based upon work supported by the National Science Foundation under grants OPP 0327440, DEB 0090202, and OPP 9911278 and the USDA under grant NRI 2004-35102-14802. Toolik Field Station meteorological data provided by James Laundre, Arctic LTER, Marine Biological Laboratory, Woods Hole, Massachusetts.

References

Arp, C. D., M. N. Gooseff, M. A. Baker, and W. Wurtsbaugh (2006), Surface-water hydrodynamics and regimes of a small mountain stream-lake ecosystem, *J. Hydrol.*, *329*, 500–513.

Bradford, J. H., J. P. McNamara, W. Bowden, and M. Gooseff (2005), Measuring thaw depth beneath peat-lined arctic streams using ground penetrating radar, *Hydrol. Processes*, *19*, 2689–2699.

Haeni, F. P. (1996), Use of ground-penetrating radar and continuous seismic-reflection profiling on surface-water bodies in environmental and engineering studies, *J. Envron. Eng. Geophys.*, *1*, 27–35.

Haury, L. R., G. B. Melbourne, and M. H. Orr (1979), Tidally generated internal wave packets in Massachusetts Bay, *Nature*, *278*, 312–317.

Hawley, N., and C. H. Lee (1999), Sediment resuspension and transport in Lake Michigan during the unstratified period, *Sedimentology*, *46*, 791–805.

Holbrook, W. S., P. Paramo, S. Pearse, and R. W. Schmitt (2003), Thermohaline fine structure in an oceanographic front from seismic reflection profiling, *Science*, *301*, 821–824.

Hutchinson, G. E. (1957), *A Treatise on Limnology*, John Wiley, New York.

Imberger, J. (1985), The diurnal mixed layer, *Limnol. Oceanogr.*, *30*, 737–770.

Johnson, C. R., W. J. O'Brien, and S. MacIntyre (2007), Vertical and temporal distribution of two copepod species, *Cyclops scutfier* and *Diaptomus pribilofensis*, in 24 hr arctic daylight, *J. Plankton Res.*, *29*, 275–289.

Jonas, T., A. Stips, W. Eugster, and A. Wuest (2003), Observations of a quasi shear-free lacustrine convective boundary layer: Stratification and its implications on turbulence, *J. Geophys. Res.*, *108*(C10), 3328, doi:10.1029/2002JC001440.

Leibold, M. A., and A. J. Tessier (1997), Habitat partitioning by zooplankton and the structure of lake ecosystems, in *Evolutionary Ecology of Freshwater Animals*, edited by B. Streit, T. Stadler, and C. M. Lively, Birkhauser, Boston.

MacIntyre, S., J. O. Sickman, S. A. Goldthwait, and G. W. Kling (2006), Physical pathways of nutrient supply in a small, ultraoligotrophic arctic lake during summer stratification, *J. Limnol. Oceanogr.*, *51*, 1107–1124.

Makino, W., T. Yoshida, H. Sakano, and S. Ban (2003), Stay cool: Habitat selection of a cyclopoid copepod in a north temperate oligotrophic lake, *Freshwater Biol.*, *48*, 1551–1562.

Olhoeft, G. R. (1981), Electrical properties of rocks, in *Physical Properties of Rocks and Minerals*, edited by Y. S. Touloukian, W. R. Judd, and R. F. Roy, pp. 257–330, McGraw-Hill, New York.

Rimmer, A., Y. Aota, M. Kmagai, and W. Eckert (2005), Chemical stratification in thermally stratified lakes: A chloride mass balance model, *Limnol. Oceanogr.*, *50*, 147–157.

Schwamborn, G. J., J. K. Dix, J. M. Bull, and V. Rachold (2002), High-resolution seismic and ground penetrating radar-Geophysical profiling of a thermokarst lake in the western Lena Delta, northern Siberia, *Permafrost Periglacial Processes*, *13*, 259–269.

Thorpe, S. A., and J. M. Brubaker (1983), Observations of sound reflection by temperature microstructure, *Limnol. Oceanogr.*, *28*, 601–613.

Wetzel, R. G. (2001), *Limnology*, Academic, New York.

Wiebe, P. H., T. K. Stanton, M. C. Benfield, D. G. Mountain, and C. H. Greene (1997), High-frequency acoustic volume backscattering in the Georges Bank coastal region and its interpretation using scattering models, *IEEE J. Oceanic Eng.*, *22*, 445–463.

Wright, D., and J. Shapiro (1990), Refuge availability: A key to understanding the summer disappearance of *Daphnia*, *Freshwater Biol*, *24*, 43–62.

J. Bradford, T. Brosten, and J. P. McNamara, Center for Geophysical Investigation of the Shallow Subsurface, Boise State University, 1910 University Drive, Boise, ID 83725, USA. (johnb@cgiss.boisestate.edu)

M. N. Gooseff, Department of Civil and Environmental Engineering, Pennsylvania State University, University Park, PA 16802, USA.

C. R. Johnson, Department of Watershed Sciences, Utah State University, Logan, UT 84322–5210, USA.